Implicit Regression in Subspace for High-Sensitivity CEST Imaging

Appendix

Contents

1 Phantom Simulation

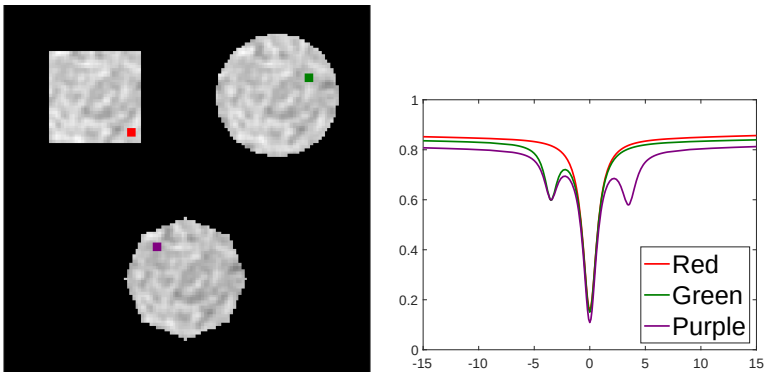

(a) Image at 0.4 ppm (b) Z-spectra at color dots

Figure 1: Synthetic phantom visualization.

We simulated three sets of z-spectra by varying the number of basis functions in the Lorentzian model [1,2] as,

$$L(\Delta\omega) = c - l_{DS}(\Delta\omega) - l_{MT}(\Delta\omega) - l_{APT}(\Delta\omega) - l_{rNOE}(\Delta\omega), \tag{1}$$

where c is a constant,

$$l_{DS}(\Delta\omega) = \frac{A_{DS}}{1 + (\frac{\Delta\omega - \delta_{DS}}{\Gamma_{DS}/2})^2}, \tag{2}$$

$$l_m(\Delta\omega) = \frac{A_m}{1 + (\frac{\Delta\omega - \delta_{DS} - \delta_m}{\Gamma_m/2})^2}, m \in \{MT, APT, rNOE\}, \tag{3}$$

where $\Delta\omega$ is chemical shift variable, c is a constant and $\delta_{MT} = -2.5ppm$, $\delta_{APT} = 3.5ppm$, $\delta_{NOE} = -3.5ppm$.

Parameter settings are shown in Table 1. The square phantom represented the direct water saturation with the MT effect, the circular phantom included extra rNOE effect, and the octagonal phantom added the APT on top of the previous two effects. In addition, we applied Gaussian filtering to the randomly generated parameters in the Lorentzian model to mimic spatial variance and smoothness, where 3×3 Gaussian kernel with $\sigma = 1$ was used.

2 In-vivo 4-pool Lorentzian Fitting

CEST mapping was achieved by 4-pool Lorentzian fitting [2,3]. The same model in Eq. 1 was applied here for addressing the following non-linear least square problem,

$$\underset{P}{\operatorname{argmin}} \frac{1}{2}||L_i(P; \Delta\omega) - Z_i(\Delta\omega)||^2, i = 1, \ldots, MN, \tag{4}$$

Table 1: Range of Randomized Parameters in MIN / MAX.

Phantom	Square	Circle	Octagon
c	0.8 / 1	0.8 / 1	0.8 / 1
δ_{DS}	0	0	0
A_{DS}	0.6 / 0.8	0.6 / 0.8	0.6 / 0.8
Γ_{DS}	1 / 2	1 / 2	1 / 2
A_{MT}	0.01 / 0.1	0.01 / 0.1	0.01 / 0.1
Γ_{MT}	80 / 80	80 / 80	80 / 80
A_{rNOE}	0	0.1 / 0.3	0.1 / 0.3
Γ_{rNOE}	-	1 / 2	1 / 2
A_{APT}	0	0	0.1 / 0.3
Γ_{APT}	-	-	1 / 2

Table 2: Boundary and initial value settings for "levenberg-marquardt" method.

Conditions	Lower Bound	Upper Bound	Initial Value
c	0.9	1	1
δ_{DS}	-0.2	0.2	0
A_{DS}	0.5	1	0.8
Γ_{DS}	1	10	6
A_{MT}	0.0025	0.2	0.1
Γ_{MT}	30	100	200
A_{rNOE}	0	0.3	0.1
Γ_{rNOE}	5	20	8
A_{APT}	0	0.4	0.3
Γ_{APT}	1	3	2

where $M \times N$ is the spatial dimension of given data, and P is the group of parameters in the Lorentzian model being estimated. The optimization problem was solved by "levenberg-marquardt" method signal by signal, of which boundary condition and initial value settings are listed in Table. 2. The optimal A_{APT} and A_{rNOE} for each pixel are then formulated to APT (3.5ppm) and $rNOE$ (-3.5ppm) maps respectively.

References

[1] Moritz Zaiss and Peter Bachert. Chemical exchange saturation transfer (cest) and mr z-spectroscopy in vivo: a review of theoretical approaches and methods. *Physics in Medicine & Biology*, 58(22):R221, 2013.

[2] Steffen Goerke, Yannick Soehngen, Anagha Deshmane, Moritz Zaiss, Johannes Breitling, Philip S Boyd, Kai Herz, Ferdinand Zimmermann, Karel D Klika, Heinz-Peter Schlemmer, et al. Relaxation-compensated apt and rnoe

cest-mri of human brain tumors at 3 t. *Magnetic resonance in medicine*, 82(2):622–632, 2019.

[3] Felix Glang, Anagha Deshmane, Sergey Prokudin, Florian Martin, Kai Herz, Tobias Lindig, Benjamin Bender, Klaus Scheffler, and Moritz Zaiss. Deepcest 3t: Robust mri parameter determination and uncertainty quantification with neural networks—application to cest imaging of the human brain at 3t. *Magnetic Resonance in Medicine*, 84(1):450–466, 2020.